Inorg. Chem. **2004**, *43*, 4862–4866

Theoretical Analysis of the Jahn–Teller Distortions in Tetrathiolato Iron(II) Complexes

Vladislav V. Vrajmasu,[†] Eckard MÜnck,* and Emile L. Bominaar*

Department of Chemistry, Carnegie Mellon University, 4400 Fifth Avenue, Pittsburgh, Pennsylvania 15213

Received April 2, 2004

Crystallographic studies of $[Fe(SR)_4]^{2-}$ (R is an alkyl or aryl residue) have shown that the $Fe^{II}S_4$ cores of these complexes have (pseudo) D_{2d} symmetry. Here we analyze the possibility that these structures result from a Jahn–Teller (JT) distortion that arises from the $e\{3z^2 - r^2, x^2 - y^2\}$ orbital ground state of Fe^{II} in T_d symmetry. Special attention is paid to the influence of the second-nearest neighbors of Fe, which lowers the symmetry and reduces the full JT effect to a smaller, pseudo JT effect (PJT). To estimate the size of the PJT distortion, we have determined the vibronic parameters and orbital state energies for a number of $[Fe(SR)_4]^{2-}$ models using density functional theory (DFT). Subsequently, this information is used for evaluating the adiabatic potential surfaces in the space of the JT-active coordinates of the FeS_4 moiety. The surfaces reveal that the JT effect of Fe^{II} is completely quenched by the tetrathiolate coordination.

1. Introduction

The structures of the coordination sites in rubredoxin (Rd)[1−5] and synthetic analogues[6−14] have been thoroughly investigated by crystallography and have recently been reviewed.[15,16] The FeS_4 cores in both the native systems and analogues display similar (pseudo) D_{2d} distortions from tetrahedral (T_d) symmetry. One of the mechanisms for breaking the T_d symmetry of the $Fe^{II}S_4$ cores in $[Fe^{II}(SR)_4]^{n-}$ complexes is the Jahn−Teller (JT) effect.[17] This possibility is supported by a number of arguments: (1) high-spin Fe^{II} has a JT-active, degenerate orbital ground state, $e\{3z^2 - r^2, x^2 - y^2\}$, in T_d symmetry; (2) similar distortions of the FeS_4 core are found in both proteins and synthetic models, as anticipated for an intrinsic effect, such as the JT effect; (3) the JT distortions of the $Fe^{II}S_4$ moiety are predicted to have the observed D_{2d} symmetry (see below); and (4) the JT distortions stabilize a $3z^2 - r^2$ ground state, which is consistent with the sign of the electric field gradient at the ^{57}Fe nucleus deduced from the Mössbauer data for rubredoxin and synthetic complexes with (pseudo) D_{2d} molecular symmetry.[18] However, there is also a number of observations that call the JT nature of the distortions into question: (1) D_{2d} distortions of the MS_4 cores in tetrathiolato metal complexes, similar to those of $Fe^{II}S_4$, have also been observed

* Authors to whom correspondence should be addressed. E-mail: eb7g@andrew.cmu.edu (E.L.B.); emunck@cmu.edu (E.M.).

[†] We dedicate this paper to the memory of our graduate student Vladislav V. Vrajmasu, who died during the preparation of this paper.

(1) Watenpaugh, K. D.; Sieker, L. C.; Jensen, L. H. *J. Mol. Biol.* **1980**, *138*, 615−633.
(2) Day, M. W.; Hsu, B. T.; Joshua-Tor, L.; Park, J. B.; Zhou, Z. H.; Adams, M. W. W.; Rees, D. C. *Protein Sci.* **1992**, *1*, 1494−1507.
(3) Archer, M.; Huber, R.; Tavares, P.; Moura, I.; Moura, J. J. G.; Carrondo, M. A.; Sieker, L. C.; LeGall, J.; Romao, M. J. *J. Mol. Biol.* **1995**, *251*, 690−702.
(4) Dauter, Z.; Wilson, K. S.; Sieker, L. C.; Moulis, J. M.; Meyer, J. *Proc. Natl. Acad. Sci. U.S.A.* **1996**, *93*, 8836−8840.
(5) Min, T.; Ergenekan, C. E.; Eidsness, M. K.; Ichiye, T.; Kang, C. *Protein Sci.* **2001**, *10*, 613−621.
(6) Holah, D. G.; Coucouvanis, D. *J. Am. Chem. Soc.* **1975**, *97*, 6917−6919.
(7) Lane, R. W.; Ibers, J. A.; Frankel, R. B.; Holm, R. H. *Proc. Natl. Acad. Sci. U.S.A.* **1975**, *72*, 2868−2872.
(8) Lane, R. W.; Ibers, J. A.; Frankel, R. B.; Papaefthymiou, G. C.; Holm, R. H. *J. Am. Chem. Soc.* **1977**, *99*, 84−98.
(9) Swenson, D.; Baenziger, N. C.; Coucouvanis, D. *J. Am. Chem. Soc.* **1978**, *100*, 1932−1934.
(10) Coucouvanis, D.; Swenson, D.; Baenziger, N. C.; Murphy, C.; Holah, D. G.; Sfarnas, N.; Simopoulos, A.; Kostikas, A. *J. Am. Chem. Soc.* **1981**, *103*, 3350−3362.
(11) Koch, S. A.; Maelia, L. E.; Millar, M. *J. Am. Chem. Soc.* **1983**, *105*, 5944−5945.
(12) Maelia, L. E.; Millar, M.; Koch, S. A. *Inorg. Chem.* **1992**, *31*, 4594−4600.
(13) Silver, A.; Koch, S. A.; Millar, M. *Inorg. Chim. Acta* **1993**, *205*, 9−14.
(14) Berg, J. M.; Holm, R. H. In *Iron−Sulfur Proteins*; Spiro, T. G., Ed.; Wiley & Sons: New York, 1982; Vol. 4, pp 1−66.
(15) Rao, P. V.; Holm, R. H. *Chem. Rev.* **2004**, *104*, 527−560.
(16) Meyer, J., Moulis, J. M., Eds. *Rubredoxin*; Wiley & Sons: Chichester, 2001.
(17) Bersuker, I. B.; Polinger, V. Z. *Vibronic interactions in molecules and crystals*; Springer-Verlag: Berlin, 1989; Vol. 49.
(18) Vrajmasu, V. V.; Bominaar, E. L.; Meyer, J.; Münck, E. *Inorg. Chem.* **2002**, *41*, 6358−6371.

10.1021/ic0400484 CCC: $27.50
Published on Web 07/10/2004

for ions with nondegenerate orbital states, e.g., for M = Mn^{2+}, Fe^{3+}, Zn^{2+}, and Cd^{2+};[10] (2) the $Fe^{II}S_4$ core of complexes with a $3z^2 - r^2$ ground state is elongated along the S_4 axis and is not compressed,[18] as predicted for a JT effect (see below); and (3) the S_4 axis of the D_{2d} symmetry of the $Fe^{II}S_4$ core coincides with the S_4 axis of the overall $[Fe(SR)_4]^{2-}$ structure, which suggests that the D_{2d} distortion of the FeS_4 moiety is not an intrinsic property of the core unit. Since the molecular symmetry of $[Fe(SR)_4]^{2-}$ is lower than T_d,[19] the e$\{3z^2 - r^2, x^2 - y^2\}$ level may already split in the case that the structure of the FeS_4 core has T_d symmetry. The splitting energy ($\Delta_{x^2-y^2}$) is then induced by the residues (R) in $[Fe(SR)_4]^{2-}$ and is non-JT in nature.[20] $\Delta_{x^2-y^2}$ weakens the JT effect, which, in the case where there is any distortion left, is called a pseudo JT (PJT) effect. To evaluate $\Delta_{x^2-y^2}$ and the vibronic parameters, we have adapted the DFT treatment of the JT effect by Bruyndonckx et al.[21] to the PJT case. Using the obtained values, we have evaluated the adiabatic potential surfaces for the ground and first excited state in the space of the JT-active coordinates of the FeS_4 unit for vanishing and nonvanishing values for $\Delta_{x^2-y^2}$. It is found that $\Delta_{x^2-y^2}$ has a profound influence on the shape of the potential surfaces from which conclusions are drawn concerning the importance of the PJT effect in tetrathiolato iron(II) complexes.

2. Methods

Density functional calculations were performed using Becke's three parameter hybrid functional (B3LYP) and basis set 6-311G provided by the Gaussian 98W (release A.9) software package.[22,23] The electron distribution was monitored by Mulliken population analysis. The SCF calculations were terminated upon reaching tight convergence criteria (10^{-6} rmsd in the density matrix and 10^{-8} au maximum deviation in energy). The calculations were performed for the models $[FeCl_4]^{2-}$, $[Fe(SCN)_4]^{2-}$, and $[Fe(SCH_3)_4]^{2-}$.

3. Results and Discussion

3.1. JT-Active Coordinates. Molecules of the form $[Fe^{II}X_4]$ (Figure 1) are Jahn−Teller active due to vibronic coupling (e ⊗ E) between the 2-fold-degenerate electronic ground configuration of the $3d^6$ high-spin metal ion (e symmetry in T_d) and the 2-fold-degenerate vibrations of the ligands, X (E symmetry in T_d). The electronic doublet consists of the doubly occupied $3z^2 - r^2$ ("z^2") and $x^2 - y^2$ components of the d^6 electronic state ^{5}e, denoted $|\theta\rangle$ and $|\epsilon\rangle$, respectively. The nature of the JT distortion can be derived as follows. The positions of the four ligands in $[FeX_4]$ are described by $3 \times 4 = 12$ spatial coordinates. There are three coordinates for the gravity center (T_2), four Fe−X bond-length expansions ($A_1 + T_2'$), and five coordinates depending on bond angles ($E + T_2''$), where the decompositions given in parentheses are in terms of irreducible representations of symmetry group T_d. The matrix elements within the degenerate electronic ground state (e in T_d) involve bra-ket combinations that transform as e ⊗ e = $a_1 + a_2 + e$. Hence, only distortions of E symmetry are Jahn−Teller active. If we assume that the gravity center of the ligands coincides with the iron position and that the four Fe−X distances are equal, the symmetry adapted coordinates for E$\{Q_\theta, Q_\epsilon\}$ and T_2''-$\{Q_\xi, Q_\eta, Q_\zeta\}$ can be expressed in terms of combinations of bond-angle distortions, $\delta_{ij} \equiv \angle X_iFeX_j - \delta_t$, as $Q_\theta = -(1/2)R_0(\delta_{12} + \delta_{34})$, $Q_\epsilon = -(1/2)\sqrt{(1/3)}R_0(\delta_{13} - \delta_{14} - \delta_{23} + \delta_{24})$ and $Q_\xi \sim \delta_{14} - \delta_{23}$, $Q_\eta \sim \delta_{13} - \delta_{24}$, $Q_\zeta \sim \delta_{12} - \delta_{34}$,[17] where $\delta_t = 109.47°$ is the tetrahedral angle and R_0 is the Fe−X distance in the equilibrium conformation. Since the sum of the six bond angle changes vanishes, $\delta_{12} + \delta_{13} + \delta_{14} + \delta_{23} + \delta_{24} + \delta_{34} \approx 0$, there is a total of five independent bond angles, spanning the space $E + T_2''$. Then, assuming that $Q_\xi = Q_\eta = Q_\zeta = 0$, we find the additional relations $\delta_{12} = \delta_{34} \equiv \delta$, $\delta_{14} = \delta_{23} \equiv \delta_1$, $\delta_{13} = \delta_{24} \equiv \delta_2 = -\delta - \delta_1$ (≡ means equal by definition) and $Q_\epsilon = \sqrt{(1/3)}R_0(\delta_1 - \delta_2)$. The latter difference can be expressed as $\delta_1 - \delta_2 = -\sqrt{(8/3)}R_0\alpha$ in terms of the tumble angle, α. The geometrical meaning of bond angle δ and tumble angle α is shown in Figure 1. The expressions for Q_θ and Q_ϵ can be simplified to

$$Q_\theta = -R_0\delta$$

$$Q_\epsilon = -\sqrt{\frac{8}{3}}R_0\alpha = -R_0\alpha' \qquad (1)$$

where we have introduced the scaled angle $\alpha' \equiv \sqrt{(8/3)}\alpha$ for the sake of conserving the aspect ratio of the potential surface plots (see below) in passing from normal coordinates (Q_θ, Q_ϵ) to angular coordinates (δ, α'). For example, in the

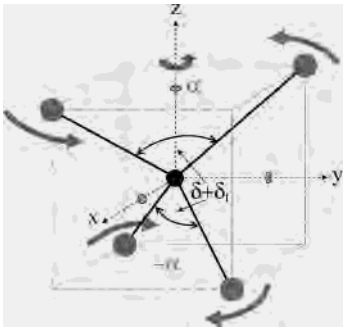

Figure 1. Tumble angle, α, and bond angle, δ, distort the T_d-symmetry of the FeS_4 unit in an $[Fe(SR)_4]$ complex and are JT active. δ_t is the tetrahedral angle, ∼109.5°. Cartesian axes used in the text for defining the 3d orbitals of iron are indicated.

(19) The majority of $[Fe(SR)_4]$ clusters has either (pseudo) D_{2d} or (pseudo) S_4 symmetry. This property is explained in the next paper of this issue.
(20) The origin of the e splitting is discussed in the next paper of this issue.
(21) Bruyndonckx, R.; Daul, C.; Manoharan, P. T.; Deiss, E. *Inorg. Chem.* **1997**, *36*, 4251−4256.
(22) Frisch, M. J.; Trucks, G. W.; Schlegel, H. B.; Scuseria, G. E.; Robb, M. A.; Cheeseman, J. R.; Zakrzewski, V. G.; Montgomery, J. A.; Stratmann, R. E.; Burant, J. C.; Dapprich, S.; Millam, J. M.; Daniels, A. D.; Kudin, K. N.; Strain, M. C.; Farkas, Ö.; Tomasi, J.; Barone, V.; Cossi, M.; Cammi, R.; Mennucci, B.; Pomelli, C.; Adamo, C.; Clifford, S.; Ochterski, J.; Petersson, G. A.; Ayala, P. Y.; Cui, Q.; Morokuma, K.; Salvador, P.; Dannenberg, J. J.; Malick, D. K.; Rabuck, A. D.; Raghavachari, K.; Foresman, J. B.; Cioslowski, J.; Ortiz, J. V.; Baboul, A. G.; Stefanov, B. B.; Liu, G.; Liashenko, A.; Piskorz, P.; Komáromi, I.; Gomperts, R.; Martin, R. L.; Fox, D. J.; Keith, T.; Al-Laham, M. A.; Peng, C. Y.; Nanayakkara, A.; Challacombe, M.; Gill, P. M. W.; Johnson, B.; Chen, W.; Wong, M. W.; Andres, J. L.; Gonzalez, C.; Head-Gordon, M.; Replogle, E. S.; Pople, J. A. *Gaussian 98*, revision A.11; Gaussian, Inc.: Pittsburgh, PA, 1998.
(23) Frisch, E.; Frisch, M. J. *Gaussian 98 User's Reference*; Gaussian, Inc.: Pittsburgh, PA, 1999.

$$\begin{pmatrix} -F\delta + \left(\frac{1}{2}K + G\right)\delta^2 + \left(\frac{1}{2}K - G\right)\alpha'^2 & F\alpha' + 2G\alpha'\delta \\ F\alpha' + 2G\alpha'\delta & F\delta + \left(\frac{1}{2}K - G\right)\delta^2 + \left(\frac{1}{2}K + G\right)\alpha'^2 + \Delta_{x^2-y^2} \end{pmatrix} \quad (2)$$

case of the rubredoxins with pseudo D_{2d}-symmetric $[Fe(SC)_4]^{2-}$ moieties, the JT-active angles have the values $\alpha \approx 0°$ and $\delta + \delta_t \equiv \angle S(1)FeS(2) \approx \angle S(3)FeS(4) \approx 104°$, so that $\angle S(1)FeS(3) \approx \angle S(1)FeS(4) \approx \angle S(2)FeS(3) \approx \angle S(2)FeS(4) \approx 112°$.

3.2. PJT Model. In a classical treatment of the nuclear motions, the solutions of the JT problem are functions of the angles δ and α'. The energy functions, $\epsilon_1(\delta, \alpha')$ for the ground state and $\epsilon_2(\delta, \alpha')$ for the excited state, define the adiabatic potential surfaces, which are obtained by diagonalizing the interaction matrix in the electronic space $\{|\theta\rangle, |\epsilon\rangle\}$ at given values for α' and δ,[17,21] shown in eq 2. The terms in eq 2 have the following meanings. $K = \langle\theta|(\partial^2 V/\partial\varphi^2)_{tet}|\theta\rangle = \langle\epsilon|(\partial^2 V/\partial\varphi^2)_{tet}|\epsilon\rangle$ ($\varphi = \delta$ or α') is the force constant of the T_d-symmetry-restoring elastic forces. The K terms in eq 2 do not affect the degeneracy of the electronic states. $F = -\langle\theta|(\partial V/\partial\delta)_{tet}|\theta\rangle$ and $G = \langle\theta|(\partial^2 V/\partial\delta\partial\alpha')_{tet}|\epsilon\rangle$ are the first- and second-order vibronic constants in the expansion of the adiabatic potential. Parameter $\Delta_{x^2-y^2}$ represents the difference between the energies for the states $|\theta\rangle$ and $|\epsilon\rangle$ at the origin, $\delta = \alpha' = 0$ and distinguishes the PJT model ($\Delta_{x^2-y^2} \neq 0$) from the JT model ($\Delta_{x^2-y^2} = 0$). We note that eq 2 represents an idealized PJT model; in the general case, the parameters may depend on the matrix element in which they occur. These dependencies are discussed in section 3.4.

3.3. Adiabatic Potential Surface for JT Case. The adiabatic potential surface for the ground state obtained for $\Delta_{x^2-y^2} = 0$ and $G = 0$ has the shape of a Mexican hat, of which the minimum is a degenerate circular manifold in the $\delta-\alpha'$ plane, with radius $R_{JT} = F/K$ and energy $-E_{JT} = -F^2/2K$. For $G \neq 0$, the circular minimum is warped by the G terms in eq 2, such that there result three degenerate minima located at $R_{JT}(\min)(1, 0)$ and $R_{JT}(\min)(-1/2, \pm(1/2)\sqrt{3})$ (Figure 2A). These minima correspond to D_{2d}-deformed conformations, with S_4 axes directed along the Cartesian axes in Figure 1; for example, the minimum on the δ axis of Figure 2A is associated with a conformation of which the S_4 symmetry axis is directed along z in Figure 1. Minimization of the function $\epsilon_1(R\cos\phi, R\sin\phi)$, with respect to radius R, yields a ϕ-dependent solution, $R = R(\phi)$, and defines a one-dimensional energy function, $\epsilon_1(\phi) = \epsilon_1(R(\phi)\cos\phi, R(\phi)\sin\phi)$. This function is periodic and has three minima (at $\phi = 0°, 120°, 240°$) and three maxima (at $\phi = 60°, 180°, 300°$). The maxima of the one-dimensional function, $\epsilon_1(\phi)$, are saddle points of the two-dimensional function, $\epsilon_1(\delta, \alpha')$. The two types of stationary points are located at different distances from the origin, namely at $R_{JT}(\min) = F/(K - 2|G|)$ and $R_{JT}(\text{saddle}) = F/(K + 2|G|)$, and have the energies $E_{JT}(\min) = F^2/(2K - 4|G|)$ and $E_{JT}(\text{saddle}) = F^2/(2K + 4|G|)$. Obviously, the largest stabilization is attained in ϕ directions for which the effective force constant is a minimum, i.e., for $K_{eff} = (1/2)K - |G|$. The energy difference between the saddle points and the minima is $\Delta_G = 4E_{JT}|G|/(K + 2|G|)$. The potential surface for the excited state, $\epsilon_2(\delta, \alpha')$, has a single minimum that is located at the origin (Figure 2B). In the following paragraph we compare this theoretical model with the results of DFT theory.

To estimate the propensity of high-spin Fe^{II} to exhibit JT distortions in a tetrahedral coordination, we have performed DFT calculations for the model complex $[FeCl_4]^{2-}$. Geometry optimization of the B3LYP/6-311G energy for $[FeCl_4]^{2-}$ results in a compressed D_{2d} structure ($\delta = +4.5°$), with an electronic ground state in which the z^2 orbital is doubly occupied, $^5A_1(z^2)$ (Table S.1). To verify that it concerns a true JT distortion, we have also performed geometry optimizations for the anions $[GaCl_4]^{1-}$ ($3d^{10}$), $[ZnCl_4]^{2-}$ ($3d^{10}$) and $[FeCl_4]^{1-}$ ($3d^5$) (Table S.1). These complexes share a tetrachloride coordination with $[FeCl_4]^{2-}$ but are JT inactive because they have nondegenerate orbital ground states. The optimized geometries of the three nondegenerate ions have undistorted T_d symmetry and confirm that the D_{2d} distortion in $[FeCl_4]^{2-}$ is a JT effect, arising from the degenerate ground state in this complex. The state $^5B_1(x^2 - y^2)$ has a D_{2d} equilibrium conformation that is elongated along the S_4 symmetry axis.[24] The distortions ($^5A_1$ compressed, $^5B_1$ elongated) are as anticipated, considering that electrons in z^2 and $x^2 - y^2$ donate charges to the areas around the z axis and the xy plane, respectively.

The symmetry along the δ axis in Figure 2 is D_{2d} and forbids orbital mixing of z^2 and $x^2 - y^2$, and consequently, the corresponding multielectronic states $^5A_1$ and $^5B_1$ do not interact either. The B3LYP/6-311G energies of these states have been presented in Figure 2C as a function of δ.[25] The two branches in Figure 2C represent sections of the energy surfaces in Figure 2A, B. The minimum and the saddle point on the δ axis in Figure 2A can be identified with the minima of the $^5A_1$ and $^5B_1$ potentials in Figure 2C, respectively; the minimum in Figure 2B corresponds with the intersection of the curves in Figure 2C.

The parameters K, G, and F (eq 2) can be extracted from an analysis of the one-dimensional section of the potential surfaces for $^5A_1$ and $^5B_1$ along the δ axis.[21] These functions can be identified with the JT energies $\epsilon_1(\delta,0)$ and $\epsilon_2(\delta,0)$, which are given by the diagonal elements of eq 2. The DFT potential surfaces in Figure 2C can be reliably fitted with the expressions $c_2\delta^2 - c_1\delta$ ($^5A_1$) and $c_2'\delta^2 + c_1'\delta$ ($^5B_1$) and yield the model parameters, $K = c_2 + c_2' = 9.28\ cm^{-1}/deg^2$, $G = (c_2 - c_2')/2 = -1.31\ cm^{-1}/deg^2$ and $F \approx c_1 \approx c_1' \approx (c_1' + c_1)/2 \approx 33.3\ cm^{-1}/deg$ for $[FeCl_4]^{2-}$. These values

(24) The state $^5B_1$ was obtained from reference state $^5A_1$ by transferring an electron from β-HOMO z^2 to β-LUMO $x^2 - y^2$ and iteration until self-consistency was reached. The equilibrium conformation for $^5B_1$ was obtained from a D_{2d}-symmetry-restricted geometry optimization.

(25) The Fe−Cl distances used in Figure 2C for $^5A_1$ and $^5B_1$ are independent of δ and obtained from geometry optimization (Table S.1).

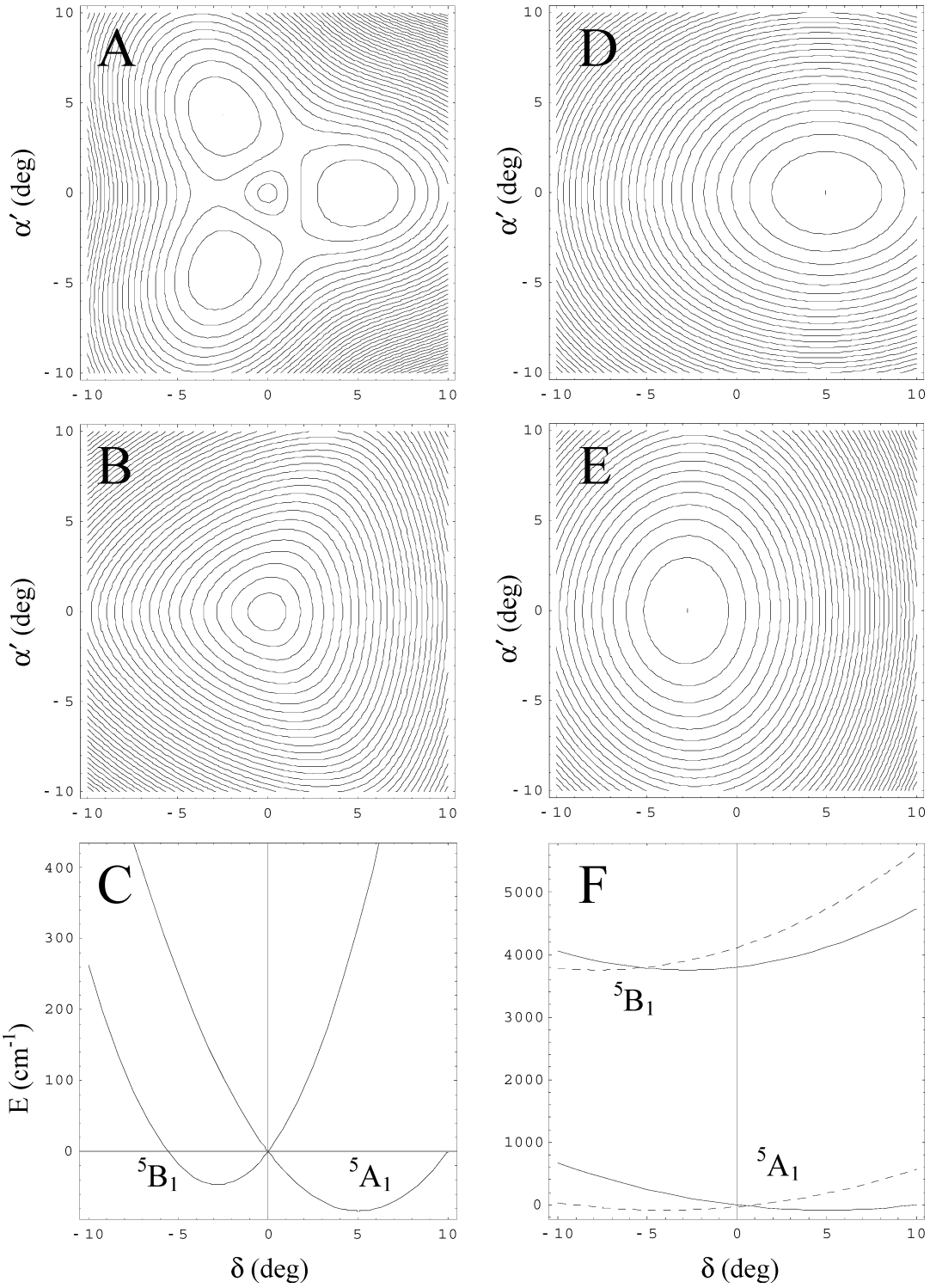

Figure 2. Equipotential curves describing adiabatic potential surfaces, $\epsilon_1(\delta,\alpha')$, for the ground state of eq 2 (A and D) and for the excited state, $\epsilon_2(\delta,\alpha')$ (B and E). Parameters used, $K = 9.3$ cm^{-1}/deg^2, $G = -1.3$ cm^{-1}/deg^2, and $F = 33.3$ cm^{-1}/deg, are obtained from analysis of DFT results for $[FeCl_4]^{2-}$ in Figure 2C. $\Delta_{x^2-y^2} = 0$ in A, B, and C; $\Delta_{x^2-y^2} = 3800$ cm^{-1} in D, E, and F. The solid curves in C and F represent sections of the potential surfaces along the δ axes in the same column. The broken curves in F are the result of DFT calculations in D_{2d} structures for the states indicated. In C, the DFT curves coincide with the solid curves. A, B, and C describe the JT effect in $[FeCl_4]^{2-}$; D, E, and F represent the case of the vanishing PJT effect in $[Fe(SR)_4]^{2-}$. The displacement of the broken curves in F relative to the solid ones is due to the term $F'\delta$ described in the text.

have been used in the calculation of Figure 2 and yield $\delta_{min} = +5.0°$, $\delta_{saddle} = -2.8°$, $E_{JT}(min) = 83$ cm^{-1} and $\Delta_G = 38$ cm^{-1}. The values of c_1 and c_1', although required to be equal by the JT model, are actually found to be slightly different (by ~6%). The difference, however, has only a minor impact on the potential surfaces: the vibronic model provides a consistent description of the DFT results for $[FeCl_4]^{2-}$.

As the values for $E_{JT}(min)$ and Δ_G are small, it is not surprising that the intrinsic D_{2d} conformation of $[FeCl_4]^{2-}$ is distorted to a variable degree under the influence of the

various crystalline hosts used in the X-ray structure determinations of this molecular anion.[26] For this reason, a comparison with crystallographic structure data has not been attempted.

3.4. Adiabatic Potential Surface for the PJT Case. Let us now consider the structure of the FeS_4 unit in complexes of the form $[Fe(SR)_4]^{2-}$. DFT calculations for a D_{2d}-symmetric structure with tetrahedral $\angle S_iFeS_j$ bond angles result in a nondegenerate $^5A_1(z^2)$ ground state and a $^5B_1(x^2 - y^2)$ excited state, located at $\sim$3800 cm^{-1} for R = CN and $\sim$3000 cm^{-1} for R = CH_3. Since the vibronic interactions in eq 2 vanish for a T_d-symmetric FeS_4 core, the energy splitting can only arise from the nonvibronic interaction, $\Delta_{x^2-y^2}$ (eq 2 for $\delta = \alpha = 0°$). By substituting $\Delta_{x^2-y^2} = 3800$ cm^{-1} and the values of K, G, and F for $[FeCl_4]^{2-}$ into eq 2, we obtain the adiabatic potential surfaces in Figure 2D, E for the ground and excited state, respectively. Comparison with Figure 2A, B shows that the introduction of $\Delta_{x^2-y^2}$ has drastically changed the shapes of the surfaces. The surfaces with three and one minima for the ground and excited states, respectively, obtained in the degenerate case are transformed into sheets with one minimum each. The $\Delta_{x^2-y^2}$ interaction in the tetrathiolato iron(II) complex has quenched vibronic mixing by the off-diagonal elements in eq 2 to the extent that the minima with $\alpha' \neq 0$ (Figure 2A) have vanished (Figure 2D). The potential surfaces in Figures 2D, E represent the common, nondegenerate case in which different electronic states give rise to different equilibrium conformations. We verified that the PJT distortions already vanish for $|\Delta_{x^2-y^2}| > 400$ cm^{-1}; since the $\Delta_{x^2-y^2}$ values for the class of $[Fe(SR)_4]^{2-}$ complexes with S_4 symmetry fulfill the inequality, the S_4 systems are not JT-active either.[27]

Despite the dissimilarity in the two-dimensional potential surfaces for the JT and PJT cases, the one-dimensional sections along the δ axis differ only by the vertical displacement $\Delta_{x^2-y^2}$ of the potential energy curve for $^5B_1$.[28] This suggests a determination of the parameters K, G, F, and $\Delta_{x^2-y^2}$ by DFT, in analogy with the JT case described in section 3.3. The broken curves in Figure 2F represents the B3LYP/6-311G energies of the states $^5A_1$ and $^5B_1$ of $[Fe(SCN)_4]^{2-}$ in D_{2d} symmetry as a function of δ. As for the chloride complex (Figure 2C), the plot consists of two parabolic curves with effective force constants $K_e(^5B_1) > K_e(^5A_1)$ ($K_e(^5\Gamma) = {}^1/_2K \pm G$) and minima $\delta_{min}(^5B_1) < \delta_{min}(^5A_1)$ that are separated by 5.4° (compared to 7.8° in the chloride). However, unlike in the case of the chloride complex, the value $\delta_{min}(^5A_1) = -3.8°$ is negative and corresponds to an elongated structure. The distortion $\delta_{min}(^5A_1) < 0$ of the geometry optimized structure for the z^2 state is in agreement with the X-ray data[16] for reduced rubredoxin and model complexes that have a z^2 ground state.[18] However, the distortion is incompatible with eq 2 because the energy versus δ plots cannot be simultaneously fitted by the expressions for the diagonal elements of the matrix (solid curves in Figure 2F). Fitting of the DFT curves requires the introduction of two independent coupling parameters, F_{z^2} and $F_{x^2-y^2}$. With this extension, the curve fits yield the values $K = 12.0$ cm^{-1}/deg^2, $G = -0.95$ cm^{-1}/deg^2, $\Delta_{x^2-y^2} = 3000$ cm^{-1}, $F_{z^2} = -32.0$ cm^{-1}/deg, and $F_{x^2-y^2} = 119.3$ cm^{-1}/deg for $[Fe(SCN)_4]^{2-}$. Apparently, the idealized PJT model, according to which $F_{z^2} = F_{x^2-y^2}$, provides an incomplete description of the DFT results for $[Fe(SR)_4]^{2-}$. There appears to be an additional interaction at the DFT level of description, one that shifts the potential wells of the two states toward negative δ. This interaction can be modeled by adding the term $F'\delta$ to the diagonal elements in eq 2, so that the effective coupling constants are given by $F_{z^2} = -F' + F$ and $F_{x^2-y^2} = F' + F$. Using the fit values for these parameters, we obtain $F = 43.7$ cm^{-1}/deg and $F' = 75.7$ cm^{-1}/deg for $[Fe(SCN)_4]^{2-}$. The K, G, and F values for the chloride complex are similar to those for the cyanide complex and have been retained in Figure 2D−F.

4. Conclusion

The distortions of the FeS_4 units in tetrathiolato iron(II) complexes are not the result of a PJT effect. DFT geometry optimizations of $[Fe(SR)_4]^{2-}$ models yield distortions of the FeS_4 units that are similar to those observed in crystallographic structures. These results suggest that the idealized PJT model in eq 2 should be extended with an additional term, $F'\delta$, to be able to describe the stereochemistry of the tetathiolato iron(II) complexes. The physical origin of this term is discussed in the next paper of this issue.

Acknowledgment. This research was supported by National Science Foundation Grant MCD 9416224 (E.M.).

Supporting Information Available: Geometry optimizations of $[MCl_4]^{n-}$. This material is available free of charge via the Internet at http://pubs.acs.org.

IC0400484

(26) Cotton, F. A.; Murillo, C. A. *Inorg. Chem.* **1975**, *14*, 2467−2469.
(27) The excited states are discussed in the next paper of this issue.
(28) This follows from inspecting the functions $\epsilon_{1,2}(\delta, 0)$, which are given by the diagonal elements in eq 2.